Effect of Compatibilizer Molecular Weight and Maleic Anhydride Content on Interfacial Adhesion of Polypropylene–PA6 Bicomponent Fibers

D. GODSHALL,[1] C. WHITE,[2] G. L. WILKES[1]

[1] Polymer Materials and Interfaces Laboratory, Chemical Engineering Department, Virginia Polytechnic and State University, Blacksburg, Virginia 24060

[2] CAMAC Corporation, Research and Development Department, Bristol, Virginia 24203

Received 9 October 2000; accepted 16 November 2000

ABSTRACT: The overall goal of the current research was to produce a bicomponent fiber consisting of a isotactic polypropylene sheath and a nylon-6 core that would be suitable for use in a pigmented carpeting application. To accomplish this, such bicomponent fibers were produced, and *in situ* reactive compatibilization was achieved using a maleic anhydride–functionalized polypropylene (PP–MA) at the interface. Bicomponent fibers with a side-by-side configuration were also spun as part of the investigative process. The adhesion of the materials at the interface and, therefore, the wear characteristics of the fibers were found to depend strongly on the molecular weight and the maleic anhydride content of the functionalized polypropylene. The wear properties and the quality of interfacial adhesion were characterized using optical microscopy to observe fiber cross sections and by accelerated wear testing of carpet samples. Differential scanning calorimetry, capillary rheometry, and tensile testing allowed for additional characterization of the materials in order to explain the differences noted in fiber performance. © 2001 John Wiley & Sons, Inc. J Appl Polym Sci 80: 130–141, 2001

Key words: bicomponent fiber; isotactic polypropylene; nylon 6; fiber spinning; maleic anhydride compatibilizer

INTRODUCTION

Bicomponent fibers offer several advantages over monocomponent fibers. In a core–sheath configuration a bicomponent fiber can display both the surface properties of the sheath material and the mechanical properties of the core material. Although blending two polymers often produces properties intermediate to the original materials, the pure-material characteristics of each polymer are retained in a bicomponent fiber. The two most commonly used materials in carpeting applications today are nylons (nylon 6 [PA6] and nylon 6,6) and polypropylene (PP). Nylon materials are used extensively in carpeting because of their excellent wear characteristics, leading to long carpet life.[1] Unfortunately, the polar nature of nylon materials causes them to readily accept the acidic stains commonly found in foodstuffs. The process of sulfonation[1] is used to increase the stain resistance of nylon materials, though the process adds expense to the material cost. Because polypropylene, is nonpolar in nature, it has excellent acid-stain resistance and can be melt-pigmented. However, polypropylene carpets are considered to have wear properties inferior to those of nylon. An

Correspondence to: G. L. Wilkes (gwilkes@vt.edu).

Journal of Applied Polymer Science, Vol. 80, 130–141 (2001)

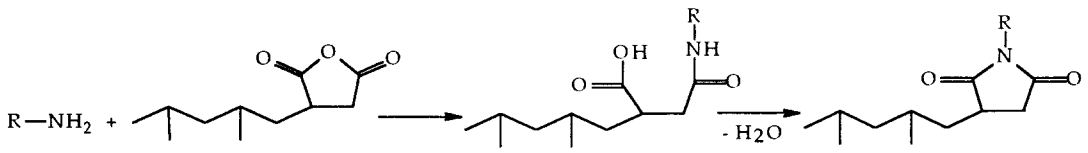

Scheme 1 Compatibilization reaction showing a maleic anhydride functionality on a polypropylene chain reacting with an amine end group of a polyamide chain.

ideal carpet fiber would combine the best of each of these polymers' properties. Thus, a melt-pigmented polypropylene sheath, nylon-6 core fiber would be an improvement over conventional monocomponent nylons or polypropylene fibers.

The same chemical differences that give PA6 and PP very different stain resistances also cause them to be incompatible. Because PA6 is polar and PP is nonpolar, these high-molecular-weight molecules will not be miscible. In order to produce a bicomponent fiber from these materials that would have sufficient interfacial adhesion to withstand drawing and service wear, a compatibilizer must be used. One possible option is the use of a maleic anhydride–grafted polypropylene material (PP–MA) in order to produce compatibilization *in situ* during the spinning process. Much work has been done to show the effect of combining PP–MA, PP, and PA6 together to improve the compatibility of PP–PA6 blends.[2–8] The mechanism of compatibilization involves the formation of a graft copolymer—consisting of a PP–MA chain chemically linked to a PA6 chain—at the PP–PA6 interface. The principal reaction mechanism[10] that is thought to proceed in the melt is shown in Scheme 1.

The reaction involves the combination of a maleic anhydride functionality with the amine end group of a PA6 chain. It is likely that the amide linkage formed proceeds by cyclodehydration to an imide linkage because of the elevated temperatures in the melt. The graft copolymer formed by this reaction resides preferentially at the interface where it was produced. At the interface the polypropylene-based portion of the graft copolymer may entangle with the PP portion of the fiber, while the nylon-6-based section can entangle with the PA6 portion of the fiber. Obviously, two important variables affecting the strength of the interface obtained through compatibilization will be the molecular weight of the graft copolymer and the maleic anhydride content of the PP–MA material.[9,10] Adequate molecular weight is necessary for both portions of the graft copolymer to form entanglements on both sides of the interface. Sufficient maleic anhydride content is necessary to provide adequate quantities of compatibilizer chains. The present study aimed at understanding how the content of the PP/PP–MA blend, which was used as the polypropylene portion of the polypropylene sheath/nylon-6 core bicomponent fiber, affects the fiber's wear properties. The variables studied were variations in maleic anhydride content and gross differences in molecular weight, in particular of PP–MA. Prior to spinning the core–sheath fibers and to subsequent wear testing, formulations were spun in a side-by-side configuration to provide information about the strength of the interface via observation of fiber cross sections using optical microscopy.

EXPERIMENTAL

Materials

The unsulfonated PA6 used in this study had an intrinsic viscosity of $[\eta] = 2.7$ dl/g in sulfuric acid with a moisture content no greater than 600 ppm. A nonfunctionalized polypropylene with a melt-flow index of 18 (PP18; ASTM D1238 − 230°C/2.16 kg) was also used. Functionalized polypropylenes were obtained from various suppliers. The maleic anhydride polypropylenes have been designated as follows: PP–MA-1, the functionalized material with the highest molecular weight used in this study that had a relatively high maleic anhydride content; PP–MA-2, the functionalized material with the lowest molecular weight used in this study, also with a relatively high maleic anhydride content; and PP–MA-3, with a molecular weight slightly greater than that of PP–MA-2 and containing less maleic anhydride. It is known that the PP–MA-2 and PP–MA-3 materials are made by the traditional melt functionalization process, which leads to increased degradation with increasing maleic anhydride content. Once received from the supplier, all PP–MA materials were stored in heat-sealed, moisture-resistant bags prior to processing. In all cases, an

Table I Typical Bicomponent Fiber-Processing Conditions

	Nylon Extruder	Polypropylene Extruder
Pressure	1000 psia	1000 psia
Metering pump speed	20.5 rpm	20.5 rpm
Barrel temperature–zone 1	243°C	221°C
Barrel temperature–zone 2	243°C	221°C
Barrel temperature–zone 3	249°C	238°C
Barrel temperature–zone 4	249°C	238°C
Head block[a]	260°C	260°C

[a]Head block is common to both extruders.

inorganic pigment was added to the PA6 component of the fiber to provide a visual contrast between the two components and to aid in their identification.

Fiber Spinning

All fibers were produced on CAMAC's bicomponent spin line, which consists of two 1″ extruders, two metering pumps, a bicomponent spin pack purchased from Hills Inc., a 15-ft stack with cross-air cooling, a spin-finish applicator, an anchor godet, two drawing godets, and a slow-speed winder. Extrusion temperatures and drawing conditions are delineated in Table I and Table II, respectively. The two separate melt streams enter the spin pack after first passing through the head block, which is common to both streams. At this point both melt streams are constrained to be at the same temperature. In all cases fibers were drawn on the godets to a draw ratio of three.

It is important to note that blends of the PP and PP–MA materials were prepared simply by physically mixing the pellets of each material prior to the spinning experiments. The static mixing element at the end of each extruder was relied on to provide sufficient uniformity. Tests were conducted that compared the quality of the fibers obtained using this standard procedure with fibers prepared using a more rigorous mixing procedure. This more rigorous procedure used a twin-screw extruder to prepare in advance the pellets of the blend to be used as the polypropylene component of the fiber. No differences between the standard procedure and the melt-blended pellet scheme were noted; thus it is assumed that a single mixing element provides adequate mixing of the polypropylene-based materials.

Blend Preparation—Nonspinning Experiments

Many experiments did not involve the testing of fiber specimens (capillary rheometry, tensile testing, SEM; most experiments involving DSC). When blends were used in these experiments, the PP/PP–MA materials were prepared using a twin-screw extruder. The extrudate was solidified in a water bath and then pelletized. The resulting pellets were used either as is or were pressed into films of approximately 0.2 mm thick between Teflon sheets using a hot press at 220°C for 5 min.

Optical Microscopy

Cross sections of fibers were obtained by embedding the fiber in molten wax (Eastotac® from Eastman Chemical Co.) and then after cooling microtoming the wax block containing the embedded fibers. The thin sections of wax and fiber were placed on glass slides, and the wax was dissolved in Varsol® (a mixture of various hydrocarbons from Exxon) prior to observation.

Capillary Rheometry

The shear deformation behavior of the materials and blends used was determined using a Kayeness, Inc., capillary rheometer. A die with L/D = 20 was used. The data were Rabinowitsch corrected[11] but not Bagely corrected. A melt time of 3 min was used in all instances.

Differential Scanning Calorimetry

A Seiko systems model 220 for differential scanning calorimetry (DSC) was used to characterize the melting and crystallization behavior of the materials. In all cases a heating rate of 10°C/min was used along with a nitrogen purge. The data

Table II Typical Bicomponent Fiber-Drawing Conditions

Godet	Speed	Temperature
Anchor roll	726 rpm	No temp. control
Draw roll 1	750 rpm	38°C
Draw roll 2	2250 rpm	26°C

presented have been normalized based on the sample weight.

Tensile Testing

The mechanical properties of blend materials were determined using a Instron model 4400R testing apparatus. Films of the blend materials were stamped into dog bone samples for testing. Because of the brittleness of some blends, all samples were warmed to 115°C in order to soften the materials prior to stamping, which prevented cracking of the samples during stamping. Specimens were allowed 24 h to equilibrate under laboratory conditions prior to testing. In all instances 10–12 samples of each blend were tested at a rate of 10 mm/min.

Scanning Electron Microscopy

Micrographs from scanning electron microscopy (SEM) were obtained using a Cambridge Stereoscan 200 with an accelerating voltage of 15 kV. Samples were sputter-coated with a 15-nm layer of gold. Micrographs of fracture surfaces were obtained by hand-fracturing samples that had been submersed 15 minutes in liquid nitrogen.

Wear Testing

Wear tests were conducted to determine qualitatively the degree of adhesion between the components, which helped to ascertain if the fibers were suitable as carpet material. A rectangular sample of a single-level (height ⅛ in.) loop pile carpet 25.5 in. by 8.25 in. was cut. This sample was used to line the inside of a drum into which a hexapod (a heavy metal object with six rubber "feet") was loaded. The drum was then rotated 50,000 times to simulate the conditions of foot traffic under accelerated conditions. Then the sample was removed, vacuumed to remove loose material, and visually evaluated.

Stain Testing

To test the resistance of the fibers to acidic stains, acid stain tests were conducted. An acidified solution of red dye was prepared using the following quantities of materials; 0.10 g of FD+C (Food, Drug and Cosmetics) red #40 was added to 1000 mL of distilled water. Then approximately 0.55 g of citric acid was added to produce a pH of 2.8. A ring 2 in. in diameter was placed on a single-level loop pile carpet sample and filled with 20 mL of the solution, which was worked into the carpet with a glass stirring rod. It should be noted that a loop pile carpet does not expose cut ends to the staining solution, so any stain penetration into the fibers will be a result of diffusion through the sheath (unless the sheath has been fractured or removed, e.g., during a wear test). The stain was allowed to set for 24 h prior to washing with water. After the carpet was rinsed to a point where the wash water appeared clear, the carpet was cleaned with an extraction vacuum cleaner and then allowed to dry for another 24 h. After this time the sample was visually inspected.

RESULTS AND DISCUSSION

Methodology of Studying Bicomponent Fibers

The accelerated wear test is an excellent indicator of the quality of the interfacial adhesion obtained in a bicomponent fiber. Unfortunately, the process of tufting carpet samples is time consuming. The pace of the research could be greatly increased if a method were developed to reject formulations that produced fibers with very poor or marginal interfacial strength prior to carpet production. Early in the research it was found that the strength of the interface obtained by compatibilization could be determined in a qualitative manner simply by studying fibers spun in a side-by-side configuration. The most basic test of the quality of the interface using side-by-side fibers involved the hand drawing of specimens. If the fiber split into two pieces during this simple drawing experiment, it would be obvious the interface was very weak. The second test involved the observation of fiber cross sections using optical microscopy. The cross-sectioning process stressed the interface sufficiently to induce interfacial failures in fibers with a weak interface.

When fibers of a given formulation were spun in a side-by-side configuration and did not show interfacial failures using these two test methods, the same formulation was spun as a core–sheath fiber. The strength of the interface obtained in these fibers was investigated using accelerated wear testing of carpet specimens. Thus, these two basic tests of a side-by-side configured fiber allowed many inferior formulations to be rejected prior to the carpet-tufting process.

Bicomponent Fiber Spinning

The most important material variable in the processing of bicomponent fibers is viscosity. The two

components must have sufficiently matched viscosities. A ratio of 4:1 is commonly quoted as the maximum viscosity ratio between which two materials may be successfully processed. Above this ratio it becomes very difficult to spin fibers of a side-by-side configuration because of the tendency of the molten fibers to bend on exiting the spinneret (commonly referred to as the nonzero extrudate angle, or dogleg). Within the spinneret capillary, the portion of the spin pack where the two polymers are in contact, an asymmetric velocity profile is established, which results from the differing viscosities of the two materials. On exiting the spinneret, the conditions of shear generated by the walls of the capillary are removed. The material within the fiber then attempts to form a flat velocity profile. For this to occur, the more viscous polymer must accelerate while the less viscous polymer must decelerate. This action causes the fiber to bend toward the half of the fiber consisting of the more viscous component.[12] Above a viscosity ratio of 4:1, the angle of bending is sufficient to cause the fiber to contact the face of the spinneret. Additional problems arise from interface movement within the spin pack as there will be a natural tendency for the lower-viscosity polymer to encapsulate the higher-viscosity polymer.[13,14] These complications associated with bicomponent fiber spinning make the characterization of the rheological properties of the materials an essential step in the bicomponent fiber-spinning process. Because viscosity is a strong function of molecular weight, rheometry can also be used to give an indication of the relative molecular weights of the species (for those with identical chain backbones). Figure 1 presents capillary rheometry data at temperatures and shear rates applicable to the spinning process. From Figure 1 it can be seen that over the shear rates tested, PA6 has the highest shear viscosity of all the materials used. It can also be seen that the PP–MA-1 material has a shear viscosity nearly that of the 18-melt-flow nonfunctionalized polypropylene in these experimental conditions. This suggests that despite the grafting of maleic groups onto the backbone, PP–MA-1 still has a substantial molecular weight. In contrast, the PP–MA-2 and PP–MA-3 materials were of such low molecular weight that satisfactory rheological data could not be obtained at processing temperatures. Therefore, the data for these two materials have been obtained at the lower temperature, 179°C, as shown in Figure 2. Despite testing at lower temperatures, these two materials have a lower viscosity than the PP–MA-1 at 243°C over the entire shear rate range tested. PP–MA-2 and PP–MA-3 do follow the typical melt functionalization trend, which causes material with a higher maleic content to have a lower molecular weight because of the degradative nature of the functionalization reaction. The low molecular weights of the PP–MA-2 and PP–MA-3 materials pose an additional problem. These materials lack sufficient melt strength to be formed into fibers, making blending with a material of a higher molecular weight a necessity. From the data in Figures 1 and 2 it is obvious that any attempts to spin a bicomponent fiber consisting of PA6 and PP–MA-2 or PP–MA-3

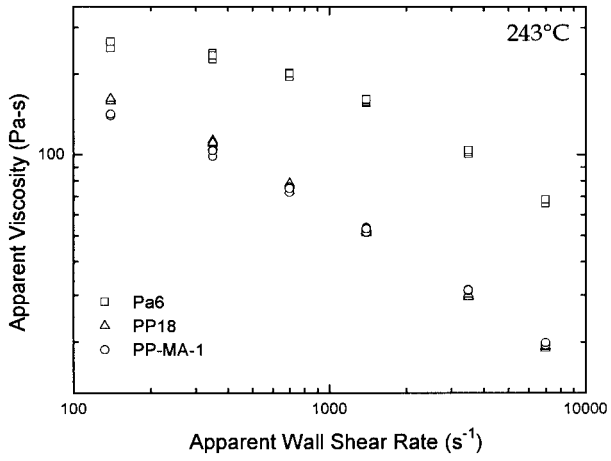

Figure 1 Plot of apparent viscosity versus wall shear rate at 243°C for PP18, PP–MA-1, and PA6 under conditions applicable to the spinning process.

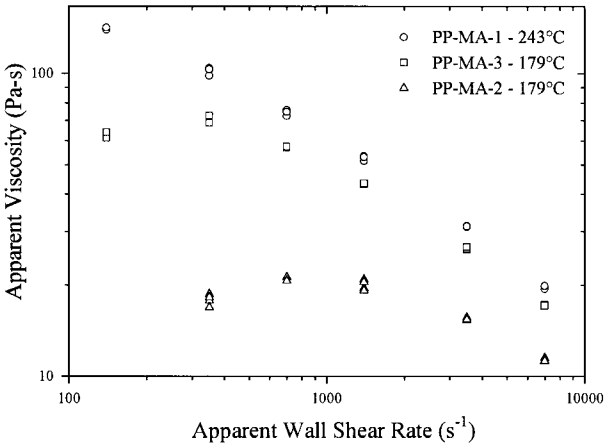

Figure 2 Plot of apparent viscosity versus wall shear rate of maleic anhydride–functionalized polypropylenes under conditions applicable to the spinning process. Note that there are two measurement temperatures.

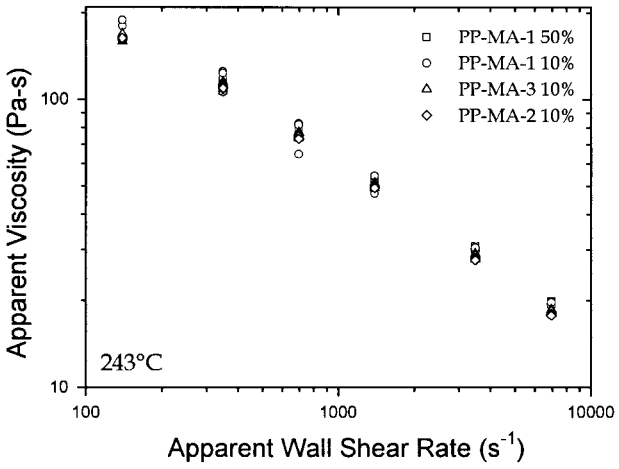

Figure 3 Plot of apparent viscosity versus wall shear rate at 243°C of blends of maleic anhydride–functionalized polypropylenes with PP18 at conditions applicable to the spinning process.

will fail because the viscosity ratios of the materials are much greater than 4:1. In order to use these materials, they must be blended with a higher-molecular-weight polypropylene to better match the viscosities of the nylon and polypropylene phases. Figure 3 shows the capillary rheometry results of such blends at temperatures and shear rates similar to those experienced during processing. The data show that small amounts of PP–MA-2 or PP–MA-3 have very little effect on the overall viscosity of the blend. At these blend levels a polypropylene phase is produced with sufficient viscosity to be melt-spun with the PA6.

Optical Microscopy of Fibers

To gain a better appreciation of the importance of viscosity matching and the level of adhesion achieved through compatibilization, initial bicomponent fibers were spun in a side-by-side configuration. Cross sections of three such fibers are shown in Figure 4. From fibers A and B it can be seen that the PA6 phase (dark portion) is more viscous than the PP/PP–MA phase (clear portion), as the less viscous component will tend to wrap around the more viscous component. An inference can be drawn from the changing shape of the interface shown in this micrograph that the capillary rheometry data is over a range of shear rates applicable to the spinning process. A calculation of the shear rate in the spinneret capillary, based on the capillary diameter and mass flow rate, gives a value of around 4840 s^{-1} at the wall. From the flow curves shown earlier it can be seen that the viscosity data obtained using capillary rheometry does predict the direction of the interface movement seen in Figure 4. Furthermore, the micrograph shows that several interfacial failures have occurred during the cross-sectioning of fiber A. Therefore, the formulations used in fibers B and C, but not fiber A, would be possible candidates for further testing as a core–sheath bicomponent fiber. The results obtained from these three fibers suggest that a relatively highly functionalized PP–MA material is necessary to produce a strong interface. The relatively low content of maleic anhydride in the PP–MA-3 material is insufficient. For this reason the PP–MA-3 material was not used in subsequent experimentation.

Representative cross sections of fibers used in carpet wear tests are shown in Figure 5. The first micrograph, in which no compatibilizer was used, emphasizes the utility of first spinning side-by-side fibers. In a core–sheath fiber it is very difficult to observe interfacial failures using this technique. The micrograph is of a fiber that apparently has a strong interface. However, later results will show that the strength of the interface obtained in this particular fiber is very poor. The final micrograph in Figure 5 raises two more issues. First, an uneven distribution of fiber sizes may be noticed. This problem occurred most often at high throughputs. It is believed that the uneven distribution of sizes was due to fluctuations in spin-line tension because of the poor quality of the slow-speed winder used. This led to an unevenness in the drawing process. Second, close observation of the cross sections reveals what appears to be a somewhat square nature to what should be perfectly round fibers. Examination of the spin pack's internals reveals that to produce a core–sheath fiber, sheath material is deposited at four points around the exterior of the core stream. These four points form the four corners of a square. It is believed that the square nature of these fibers is a result of inadequate time for the materials to completely relax to the most desired round core–sheath configuration. Once again, this problem was more noticeable at high throughputs.

Melting Behavior of Materials

A key material property in fiber applications is the crystal content of the fiber. Crystalline con-

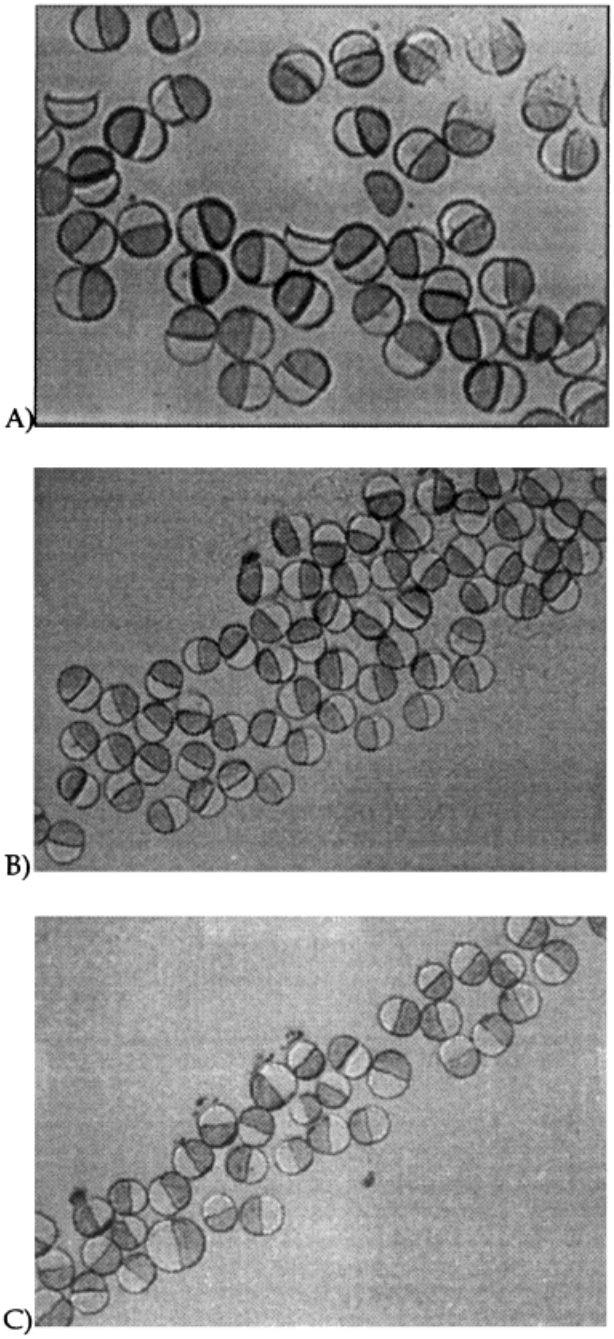

Figure 4 Bicomponent fiber consisting of 50% clear phase (PP/PP–MA portion) and 50% dark phase (PA6 portion). PP/PP–MA phase consists of (a) 10% PP–MA-3, 90% PP18, (b) 5% PP–MA-2, 95% PP18 (c) 50% PP–MA-1, 50% PP18.

tent of both the PA6 and PP portions of the fiber will influence many key properties. For example, crystallinity improves a fiber's ability to retain its shape under conditions of elevated temperature, in addition to reducing the amount of stainable material. The glass-transition temperatures of PP (−18°C[15]) and PA6 with a high moisture content (20°C @ 50% RH[16]) are at or below room temperature. Thus, if these fibers are to retain their shape when stressed, it is necessary to have sufficient levels of crystallinity to control creep. The action of friction on carpet can heat the fibers, making the need to restrict the mobility of the amorphous phase even more critical. It is important that the addition of maleic groups along the backbone of the chain does not overly disrupt the symmetry of the polypropylene chains so as to reduce the ability of the material to crystallize. Figure 6 shows DSC melting endotherms for the maleated polypropylenes used in this study along with the nonfunctionalized polypropylene. The most important trend that can be noted from the data is the ability of the materials to crystallize has not been affected by the presence of the maleic groups along the backbone of the chain. Integration of the area under each of the endotherms shows that all the materials contain roughly the same crystalline content. The results of this integration are shown in Table III. Also of interest is the small low-temperature melting peak that can be observed in the PP–MA-1 material. It is believed this peak corresponds to a small fraction of a low-density polyethylene that has been added to the material to improve its melt strength through the incorporation of long-chain branching in this component. Finally, it can be seen that the PP–MA-2 material contains what appears to be a dual melting peak. The cause of this behavior was not studied in depth. It likely involves melting recrystallization as the chains attempt to increase the perfection of the crystallites. Attempts to determine by optical microscopy if the dual melting was a result of the formation of separate PP and PP–MA crystalline phases, as had been done by Duvall et al.,[6] were unsuccessful. The corresponding crystallization behavior of these materials and blends is depicted in Figure 7. No signs of the separate crystallization of two distinct polypropylene fractions can be seen in these traces. As expected, the polyethylene component nucleates at temperatures below that of the PP. Figure 8 presents a DSC scan of a fiber with a PA6 core and a sheath containing the PP–MA-1 material. The large, broad endothermic event between 25°C and 110°C corresponds to the relaxation of stresses and the loss of orientation inherent in the fiber at the beginning of the experiment. Once again, the two characteristic melting peaks of the PP–MA-1 are evident (peaks A and B). It can be

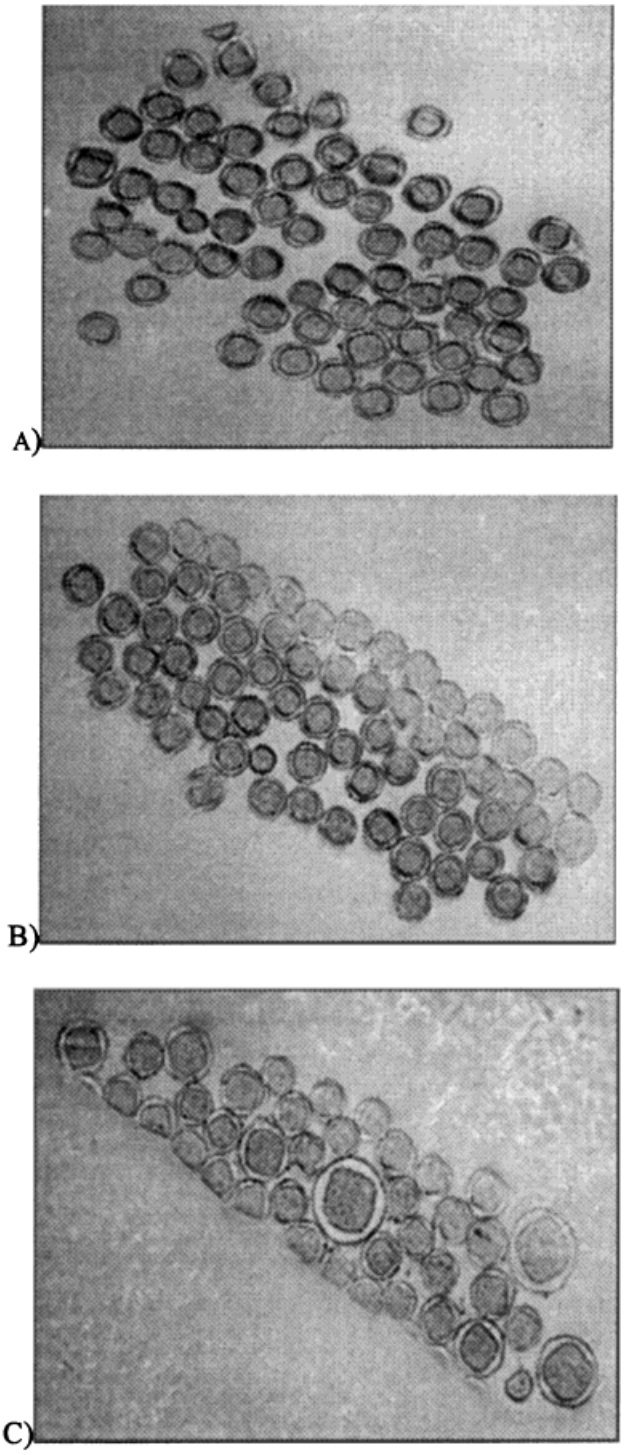

Figure 5 Cross sections of representative core–sheath fibers. All fibers consist of a 60% core of PA6 and 40% sheath of (a) PP18, (b) 10% PP–MA-2, 90% PP18, (c) 67% PP–MA-1, 33% PP18.

seen that a substantial quantity of the fiber's PA6 core was crystalline (peak C). It is doubtful that the ability of the PA6 component to crystallize would be compromised in the bicomponent spinning process, as it was blended with only a small amount (3–4 wt %) of inorganic pigment. Figure 8 confirms the prior crystallization of the PA6, suggesting that these bicomponent fibers will contain the crystallinity necessary to provide adequate mechanical properties. Additional evidence of the crystallization of both the PP and PA6 portions of these fibers is presented in Figure 9. This wide-angle X-ray scattering (WAXS) pattern of the same fiber observed in Figure 9 clearly shows reflections that can be attributed to both PP and PA6. The pattern shows the expected sign of azimuthal dependence, which also would be expected for the oriented fiber. No effort was made during the study to optimize or find the limits to which the bicomponent fibers produced could be drawn. Obviously, the amount of orientation induced in

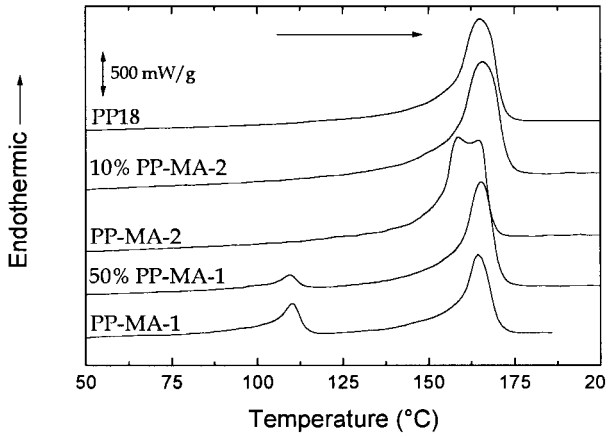

Figure 6 DSC melting behavior of several of the investigated materials and selected blends.

Table III Crystalline Content of Materials Determined Using DSC

Material	T_m (°C)	T_c (°C)	Crystallinity (%)
PP18	165.1	110	46.3
PP-MA-1	110, 164.2	96, 117.6	8.3, 31.1
PP-MA-2	158.7, 164.6	113.2	48.7
PP-MA-3	163.9	113.2	47.9
PP-MA-4	166	111.5	47.9
PP-MA-6	160.9	112.2	49.5
PE-MA	110.8	91.8	37.8

Multiple entries refer to the lower and higher melting peaks respectively. ΔH_f PP = 209 J/g, ΔH_f PE = 289.9 J/g. PP-MA-1 entry represents the percentage of crystalline PE and PP respectively.

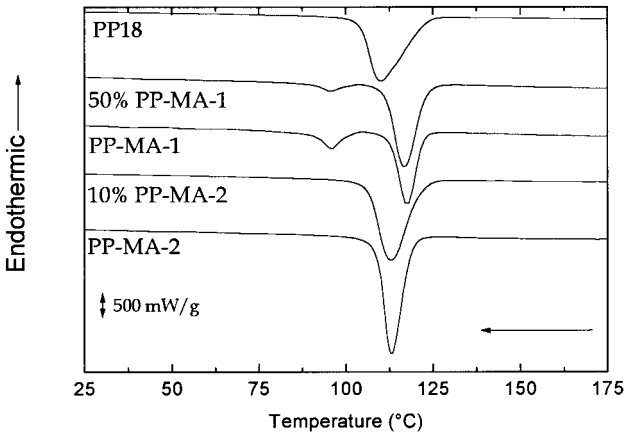

Figure 7 DSC crystallization behavior of several of the investigated materials and selected blends.

the fiber should distinctly influence its mechanical properties.

Mechanical Properties of Blends

To further understand the properties observed during wear testing of carpet samples, dog bone samples were cut from films containing the same polypropylene blend ratios as those used during fiber spinning (tests were not conducted on fiber samples). The results of these tensile tests are shown in Figure 10. Although the blends have modulus values comparable to PP18, it can be seen that for equivalent contents the PP–MA-2 material produces blends with a higher modulus than does the PP–MA-1 material. However, the PP–MA-2 blends were quite brittle. Films of these blends were not

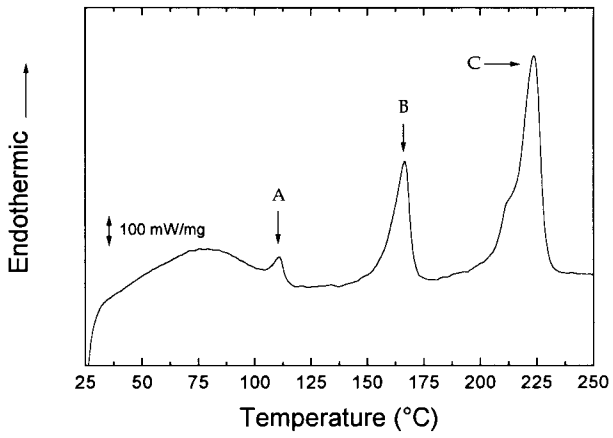

Figure 8 Melting behavior of a fiber consisting of a 50% core of PA6 and a 50% sheath of PP–MA-1.

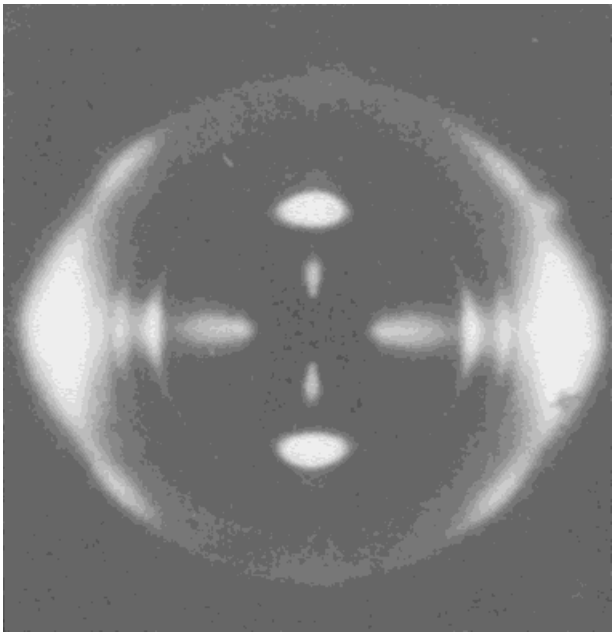

Figure 9 WAXS pattern of a fiber consisting of a 50% core of PA6 and a 50% sheath of PP–MA-1. Fiber axis is vertical.

creasable and quite fragile. A carpet fiber during its lifetime will be subjected to large strain deformations for which modulus data may not be an adequate indicator of the performance level of the fiber. This point is emphasized in Figure 11, in which the toughness properties of these blends are compared. The plot clearly shows that high PP–MA-2 contents lead to drastic reductions of toughness. Thus, although from the perspective of modulus the PP–MA-2 blends appeared to be superior, the opposite is true from a toughness standpoint. The lack of toughness of the PP–MA-2 blends is not sur-

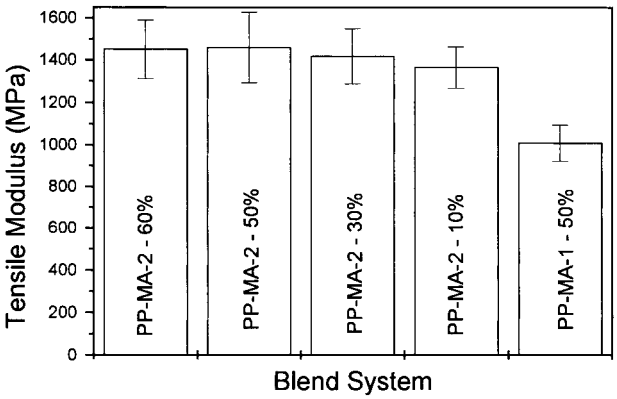

Figure 10 Tensile modulus of selected materials.

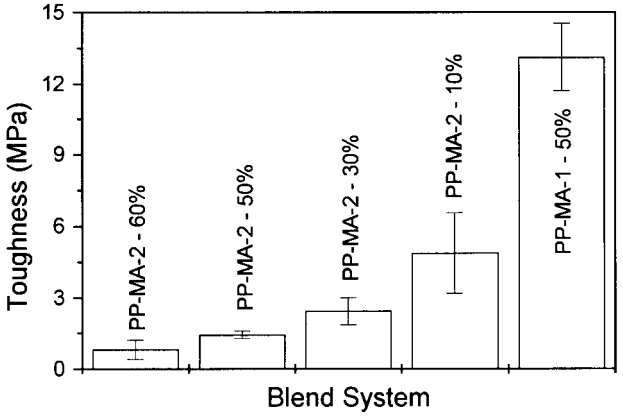

Figure 11 Toughness of selected blends.

prising considering the capillary rheometry data shown earlier. The PP–MA-2 material is of a very low molecular weight; thus it has relatively few entanglements, leading to a polymer with a very low strain to break. Because of the high degree of functionalization present in some of these materials, it is possible the poor mechanical properties are also a result of a phase-separated morphology. It is also possible that high levels of maleic anhydride grafting cause the grafted chains to become incompatible with polypropylene. As a first check of this phenomenon, fracture surfaces of these blends were examined. Dog bone samples fractured under liquid N_2 were observed using SEM, as shown in Figure 12 (note the slightly different levels of magnification). These SEM images show a phase-separated morphology in the second micrograph. However, this micrograph corresponds to the PP–MA-1 blend not the PP–MA-2. At this scale length no phase separation can be observed using SEM in the PP–MA-2 blend. Thus, to assume that the relatively poor toughness of the PP–MA-2 blends in comparison to the PP–MA-1 blends is due to morphological differences appears to be incorrect. The mechanical response of the functionalized materials appears to be a strong function of molecular weight.

Wear Testing of Carpet Samples

An indication of how a carpet fiber will perform in service can be obtained using accelerated wear testing. Several sets of core–sheath fibers were tufted into single-level loop pile carpets and were then wear-tested. The wear test exposes weaknesses in interfacial adhesion and inadequacies that may be associated with the mechanical properties of the materials. Figure 13 shows the results of a wear test on three different fibers. Severe wear shows itself in these samples through a distinct visual whitening of the fibers from the introduction of gaps at the interface, which scatter light. Thus, the compatibilization between the two halves can be measured qualitatively with the wear test. To determine the relative degree of wear on a carpet sample, the upper and lower edges of the sample (the regions where the hexapod does not trample) should be compared to the center of the sample. Visual contrast of these two regions is indicative of a carpet with poor wear characteristics. Sample A in Figure 13 is of a core–sheath fiber in which no compatibilizer was used. The arrows indicate regions not worn by the hexapod, representing the appearance of the entire specimen prior to testing. As expected, the degree of whitening is large because

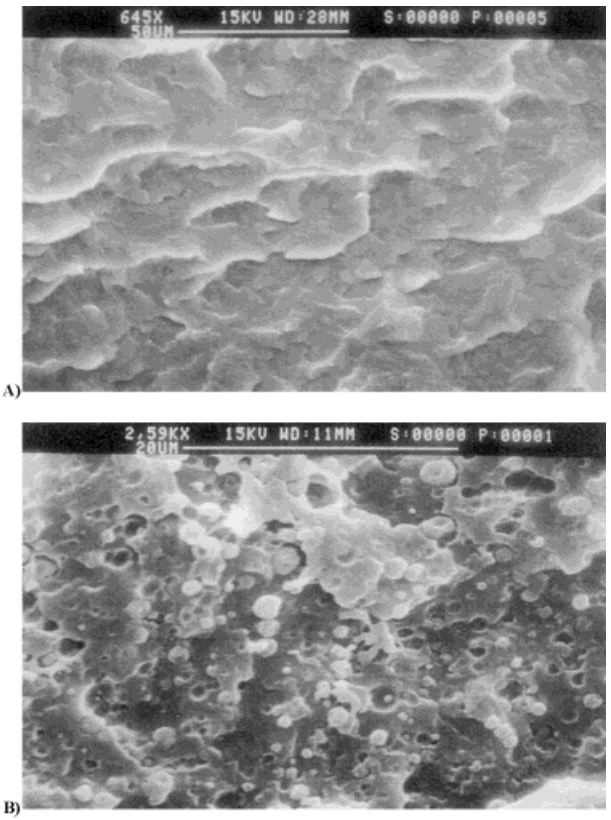

Figure 12 SEM micrographs of fracture surfaces. Blends consist of (a) 60% PP–MA-2, 40% PP18, (b) 50% PP–MA-1, 50% PP18. Note that there are slightly different magnification levels between micrographs.

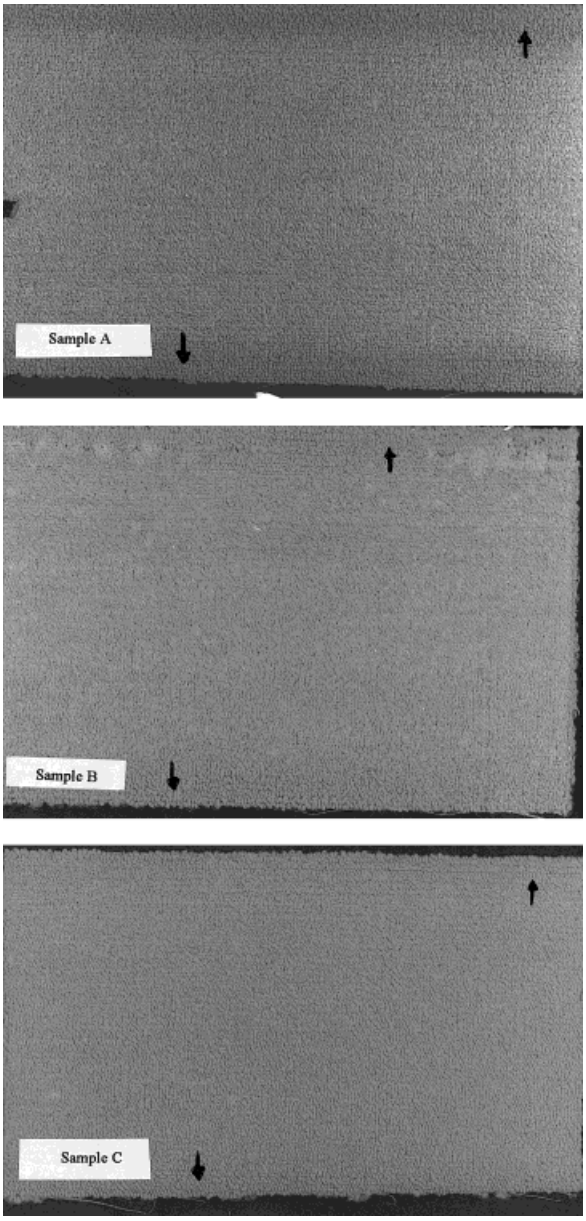

Figure 13 Results of accelerated wear testing. Samples tufted into single-level loop pile carpet from core–sheath fibers consisting of 60% core of PA6 with 40% sheath material of (a) PP18, (b) 10% PP–MA-2, 90% PP18, (c) 67% PP–MA-1, 33% PP18. Arrows point to regions that did not experience wear during testing.

there is no compatibilization. Sample B of Figure 13 shows a carpet in which the polypropylene component consisted of 10% PP–MA-2, which also shows poor wear characteristics. Cross sections of the 10% PP–MA-2 fibers when spun as side-by-side fibers showed adequate adhesion. It is believed the lack of toughness in these blends makes the use of the PP–MA-2 material unsuitable as a carpet material as it is too brittle. Sample C of Figure 13 shows excellent wear resistance. Very little, if any, contrast can be noted between the edges and center of the sample. Although the PP–MA-1 material produces blends that are not as stiff as the PP–MA-2 blends, the PA6 core is sufficient to provide resistance to matting, while the compatibilizer produces excellent adhesion between the PA6 and PP.

Stain Testing of Carpet Samples

As stated earlier, the goal of this project was to combine the wear resistance of a PA6 fiber with the stain resistance of a PP fiber. Stain testing using an acid red solution was conducted to determine if the high content of polar maleic anhydride groups in the compatibilizer was sufficient to detract from the natural acid stain resistance of the PP phase. Figure 14 shows the results of one such test. From the photograph it can be seen that these fibers have excellent stain resistance despite the presence of a number of polar functional groups on the backbone of the PP–MA material. These results are very promising, as the stain resistance obtained by a bicomponent fiber will be durable, in contrast to surface treatments whose effectiveness will diminish with time.

CONCLUSIONS

Bicomponent fibers consisting of polypropylene and nylon-6 were produced in which the inter-

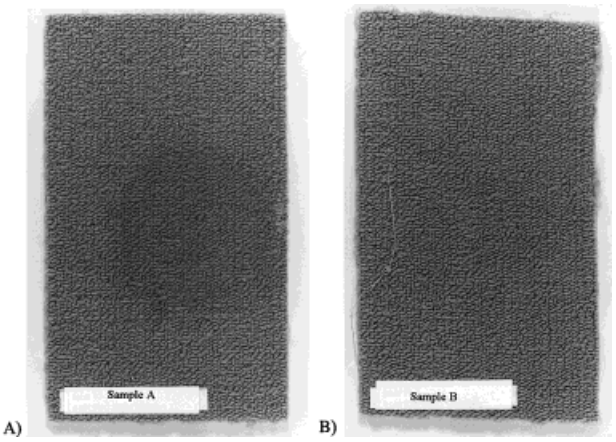

Figure 14 Acid red stain testing of carpet samples. Samples tufted into single-level loop pile carpet from fibers consisting of a 60% core of PA6 with 40% sheath material of 33% PP–MA-1, 67% PP18 (a) after staining, (b) after cleaning.

face between the two materials was strengthened through the use of an *in situ*–formed compatibilizer. This compatibilizer was formed using a maleic anhydride–functionalized polypropylene to react with the amine end groups of the nylon-6 chains, making a graft copolymer capable of entangling with both phases across the interface. It was found that the relative molecular weight and the amount of maleic anhydride content were important variables in determining the quality of the interface produced. Wear testing of core–sheath fibers and cross sectioning of side-by-side fibers provided an adequate means of rating the quality of the interfacial adhesion obtained. High contents of functionalized material of sufficient molecular weight were shown to produce a fiber that displays sufficient crystallinity, interfacial adhesion, and stain resistance to be used in carpeting applications.

REFERENCES

1. Brody, H. Synthetic Fibre Materials; John Wiley and Sons: New York, 1994.
2. Heimenz, P. C. Polymer Chemistry—The Basic Concepts; Marcel Dekker: New York, 1984.
3. Ide, F.; Hasegawa, A. J Appl Polym Sci 1974, 18, 963.
4. Bidaux, J.; Smith, G. D.; Bernet, N.; Manson, J. E. Polymer 1996, 37, 1129.
5. Li, H.; Chiba, T.; Higashida, N.; Yang, Y.; Inoue, T. Polymer 1997, 38, 3921.
6. Gonzalez-Montiel, A., Keskkula, H.; Paul, D. R.; J Appl Polym Sci, Part B: Polym Phys 1995, 33, 1751.
7. Duvall, J.; Sellitti, C.; Myers, C.; Hiltner, A.; Baer, E. J Appl Polym Sci 1994, 52, 207.
8. Boucher, E.; Folkers, J. P.; Creton, C.; Hervet, H.; Leger, L. Macromolecules 1997, 30, 2102.
9. Boucher, E.; Folkers, J. P.; Hervet, H.; Leger, L. Creton, C. Macromolecules 1996, 29, 774.
10. Al-Malaika, S. Reactive Modifiers for Polymers; Chapman and Hall: London, 1997.
11. Kramer, J.; Norton, L. J.; Dai, C.; Sha, Y.; Hui, C. Faraday Discuss 1994, 98, 31.
12. Creton, C.; Kramer, E. J.; Huim, C.; Brown, H. R. Macromolecules 1992, 25, 3075.
13. Southern, J. H.; Ballman, R. L. J Appl Polym Sci 1975, 13, 863.
14. Han, C. D. J Appl Polym Sci 1973, 17, 1289.
15. White, J. L.; Lee, B. Transactions of the Society of Rheology 1975, 19, 457.
16. Bandrup, J.; Immergut, E. H. Polymer Handbook, 2nd ed.; Wiley-Interscience: New York, 1975.
17. Kohan, M. I. Nylon Plastics; Wiley-Interscience: New York, 1973.